Ultrasound parameters of arteries and heart in normal fetuses

Guihong Chen[1], Pin Wang[1], Yanhong Zhang[1], Na Li[1], Liman Fu[1], Yu Chen[1], Xuna Geng[1], Yongfeng Han[1], Lu Qin[1], Bulang Gao[2], Tianxiao Yu[1*] and Jie Mi[2*]

Abstract

Background Currently, no normal ultrasound data of the fetuses during the 20–40 gestation have been obtained for references of fetal growth and development. If such ultrasound data existed for prenatal diagnosis of possible diseases and abnormalities, neonates would be able to get timely treatment immediately after birth. This study was thus performed to obtain ultrasound parameters of normal fetuses during the 20–40 week gestation and the distribution of ultrasound parameters with the gestational age for references of detecting potential fetal diseases and abnormalities.

Methods Normal fetuses without any abnormalities were enrolled, and the ultrasound parameters of the general biology, arteries, and aorta were measured and analyzed.

Results 417 normal fetuses were enrolled. A significant ($P < 0.05$) negative correlation with the gestational age was detected in the peak systolic velocity/peak diastolic velocity (S/D), pulsatility index (PI) and resistance index (RI) of the umbilical artery (UA). A relatively stable relationship with the gestational age was detected in the fetal weight%, S/D, PI and RI of the middle cerebral artery (MCA), peak systolic velocity (PSV) and velocity time integral (VTI) of the intra-abdominal UA, fetal heart to chest ratio, mitral valve (MV)- and tricuspid valve (TV)-E/A peak flow velocity, aortic isthmic Z-score and displacement, distance between the brachiocephalic artery-left common carotid artery (BA-LCCA) and LCCA-left subclavian artery (LSA), Z-score of aorta, ascending aorta (AAO), pulmonary artery (PA), main pulmonary artery (MPA), and descending aorta (DAO). A significant ($P < 0.05$) positive correlation with the gestational age was detected in the fetal biological data, MCA PSV and VTI, free-UA PSV and VTI and cardio-thoracic ratio, cardiac parameters, ductus arteriosus (DA) and isthmus diameter, aortic parameters, PA and MPA diameter, MPA PSV and VTI, isthmus flow volume and velocity and PA flow volume, DA and BA parameters, and LCCA and LSA parameters (flow volume, PSV, and VTI).

Conclusion A certain correlation and distribution trend is detected in the ultrasound parameters of normal fetuses, and the ratios among different parameters remain relative stable. These findings can be used for determination of abnormal growth of the fetuses in prenatal ultrasound scan.
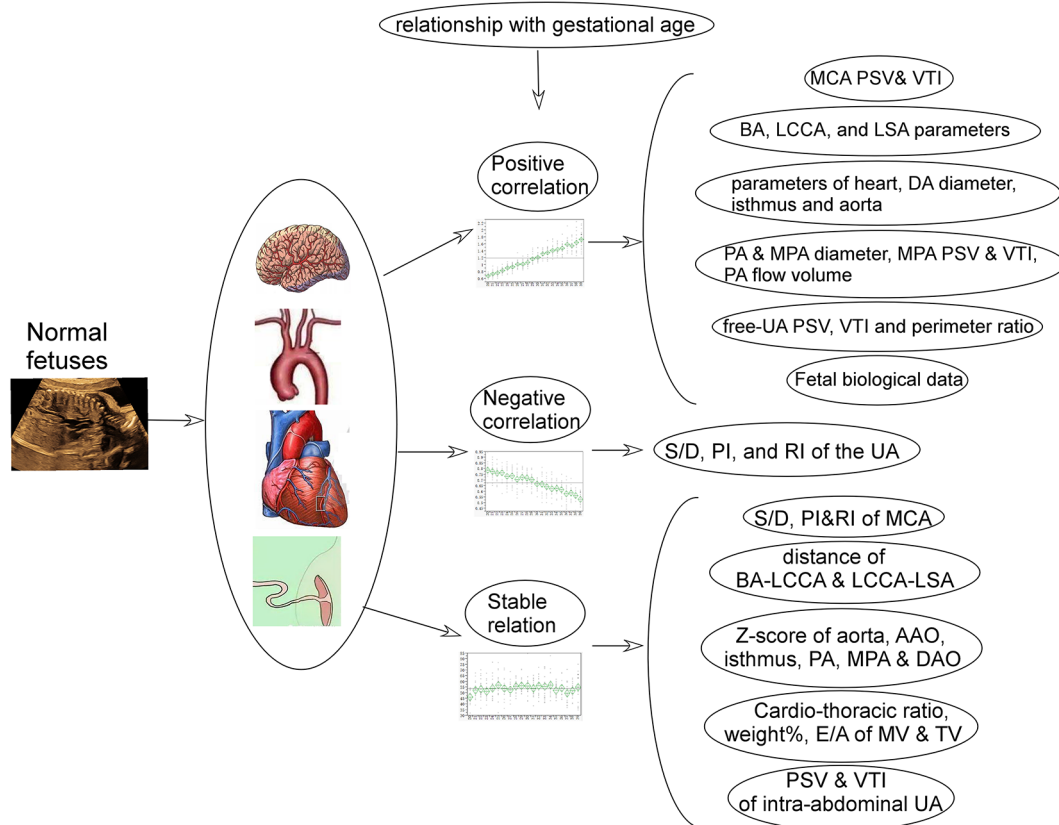
*Correspondence:
Tianxiao Yu
yutianxiao1111@163.com
Jie Mi
mmmjjj2015@163.com

Full list of author information is available at the end of the article

Graphic Abstract

Keywords Normal fetuses, Prenatal ultrasound parameter, Trend, gestational age, Image

Authors:

Introduction

Both fetal size and growth velocity (change in size with time) have been used to assess fetal growth and development abnormalities [1–10]. Use of fetal size is common, and growth velocity evaluation is also a logical approach for fetal growth determination. For growth velocity, serial measurements of the fetuses are necessary over a large range of fetal age, however, strict serial evaluation of the fetuses may be difficult and only a limited number of studies have been conducted except for studies on individualized growth assessment [11–13]. Fetal growth velocity evaluation is focused on detection of growth abnormalities, and individualized growth assessment uses growth velocity mainly for evaluation of growth potential [14]. Measurement of the second trimester growth data can be used to specify the Rossavik size models to generate the expected third trimester size trajectories and birth features [11]. Good agreement has been achieved between the actual values and the expected data in fetuses and neonates with normal neonatal growth results as proved

by the prenatal percent deviations and growth potential realization indexes in neonates [11, 14, 15]. Nonetheless, no normal ultrasound data of the fetuses during the 20–40 week gestation have been obtained for references of fetal growth and development. If such ultrasound data existed for prenatal diagnosis of possible diseases and abnormalities, neonates would be able to get timely treatment immediately after birth. This study was thus performed to obtain ultrasound parameters of normal fetuses during the 20–40 week gestation and the distribution of ultrasound parameters with the gestational age for references of detecting potential fetal diseases and abnormalities.

Materials and methods
Subjects
This prospective single-center study was approved by the ethics committee of the Fourth Hospital of Shijiazhuang with informed consent given by the pregnant women to participate. All methods were performed in accordance with the relevant guidelines and regulations. From May 2021 to May 2023, pregnant healthy women with antenatal sonography, regular menstruation, no genetic history,

no pregnancy complications, 20–40 weeks of gestational age, and healthy neonates without abnormalities confirmed after birth were enrolled. The inclusion criteria were healthy pregnant women with known last menstrual time, no abnormalities by prenatal ultrasound screening, regular menstruation, 20–40 weeks of gestational age, antenatal sonography of the fetuses, delivery in our hospital, follow-up up to 6 months after birth, and no abnormalities confirmed by sonography and postpartum follow-up. The exclusion criteria were pregnant women with irregularity of menstruation, unknown time of last menstruation, genetic diseases, pregnancy complications, infectious diseases, and multiple pregnancies.

Instruments and methods

Ultrasound scan was performed with the GE Voluson E10 Color Doppler ultrasound diagnostic instruments (General electric, Tiefenboch, AUSTRIA), quipped with 2D/3D transabdominal probes (frequency 2-5 MHz/4-8 MHz, probe model C1-6-D and RAB6-D, and power < 100 mW/cm^2), STIC software package, and 4D View 7.0 Offline analysis. Under the fetal quiet state without influencing of breathing and movement, ultrasound scan and echocardiography were conducted to evaluate fetal growth, weight, and abnormalities. All the data were measured three times to obtain the average values by an experienced ultrasound physician with over 10 years of experience (Fig. 1).

Ultrasound parameters

General biological data and ultrasound parameters were measured, including peak systolic velocity (PSV), pulsatility index (PI), resistance index (RI), S/D ratio (between the peak systolic velocity and peak diastolic velocity) and velocity time integral (VTI) of the middle cerebral artery (MCA) and umbilical artery (UA, both inside and outside the fetal abdomen before UA placental insertion). The heart axis, cardio-thoracic ratio (Area/Circumference), right and left atrium (end systole) and ventricle (end diastole) dimension, mitral valve A-peak flow velocity (MV-A), mitral valve E-peak flow velocity (MV-E), tricuspid valve A peak (TV-A), and tricuspid valve E peak (TV-E),
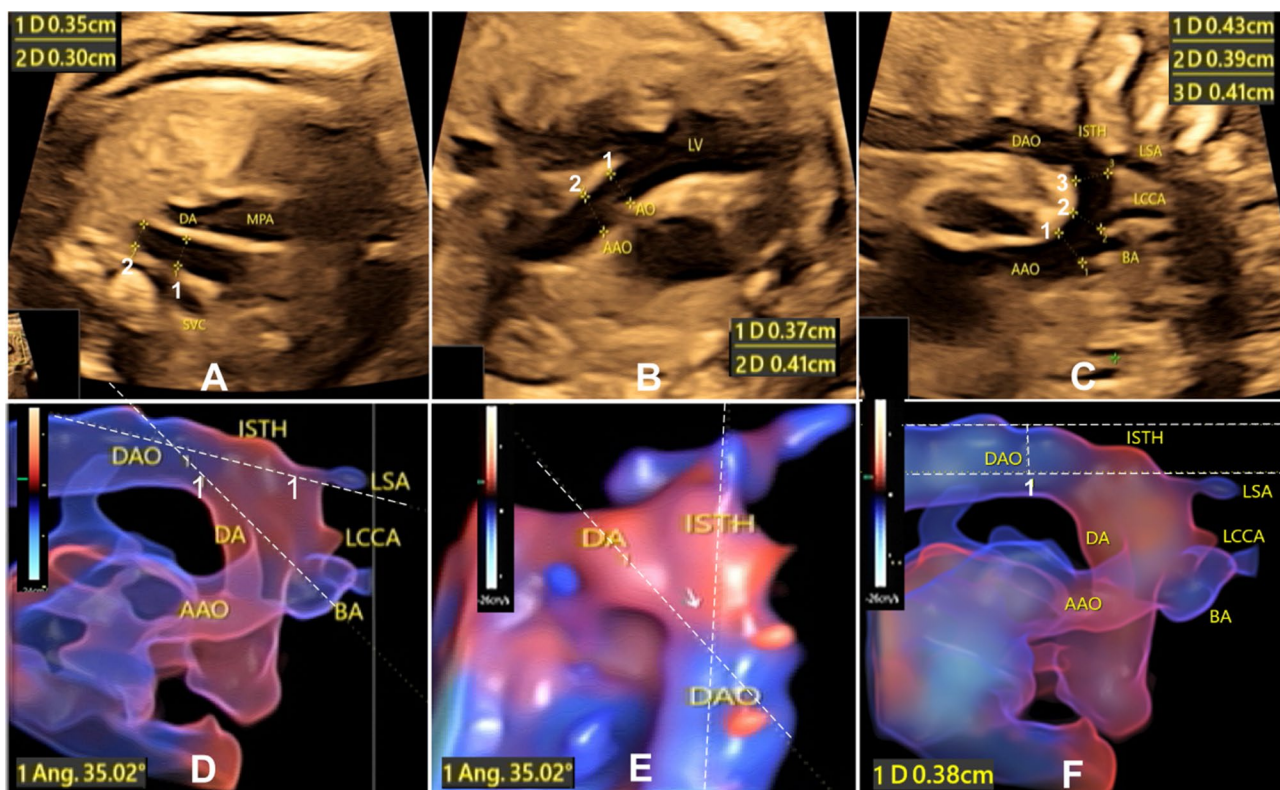

Fig. 1 Parameters measured on ultrasound images. **A**. The diameters of the transverse aorta (1) and the aortic isthmus (2) were measured on the 3 vessel trachea view, with the transverse aorta diameter of 0.35 cm and the isthmus diameter of 0.30 cm. **B**. The diameter of the aorta (AO) at the aortic valve annulus and the ascending aorta (AAO) was measured at the left ventricular outflow tract section, with the AO diameter (1) of 0.37 cm and the AAO diameter of 0.41 cm. **C**. The diameter of the aortic arch was measured at three locations: arch 1 before the brachiocephalic artery (BA), arch 2 before the left common carotid artery (LCCA) and arch 3 before the left subclavian artery (LSA). **D**. The ductus arteriosus (DA)-isthmus angle was measured on the HD Live Flow image on the sagittal view, with the DA-Isthmus angle of 35.02°. **E**. The DA-isthmus angle was measured on the HD Live Flow image viewed from the bird's eye's view, with the DA-Isthmus angle of 35.02°. **F**. The displacement (or distance) from the LSA origin to the DAO outer edge were measured on the 3D STICK-HD Live Flow image. MPA, main pulmonary artery; SVC, superior vena cava; ISTH, aortic isthmus

were measured in the four-chamber view. Systolic aortic valve annular diameter, ascending aortic (AAO) inner diameter, aortic flow velocity and volume, pulmonary valve annular diameter, main pulmonary artery (MPA) inner diameter, and pulmonary artery (PA) flow velocity and volume were measured at the left and right ventricle outflow tract sections, with the spectrum automatic envelope to get the respective VTI and immediate heart rate. The left (LCO) and right (RCO) cardiac output, and combined cardiac output (CCO=LCO+RCO) were calculated according to the formula $Q=(D/2)^2$ x 3.14 x VTI x HR (immediate heart rate). The diameter of ductus arteriosus (DA), transverse arch, and aortic isthmus was measured at the tracheal section of three vessels (3VTV). In the sagittal view of the aortic arch, the diameter of the aortic arch at three locations of arch 1–3, isthmus, descending aorta (DAO), three arch branches, the distance between the arch branches at the starting part, and the flow parameters were measured. The ratios among the parameters were calculated. The real-time 3D STIC mode was selected for 3D scanning. In the Color Render mode, the HD live flow imaging mode was applied to obtain the 3D image of the long axis of the aortic arch and catheter arch for relevant parameters (Fig. 1).

Statistical analysis

The JMP software (10.01.2, SAS Institute, Cary, NC, USA) was used for the statistical analysis. Continuous measurement data meeting the normal distribution requirement were presented as mean and standard deviation or as median and interquartile range if not meeting the normal distribution. Categorical data were expressed as frequency and percentage. The Chi square analysis was performed for the relationship of ultrasound parameters with the gestational age, with the R^2 and F ratio calculated. The significant P value was set at <0.05.

Results

417 normal fetuses without any abnormalities were enrolled, and the ultrasound parameters of the fetal general biology, MCA, UA, DA, aortic isthmus, aorta, aortic arch, arch arterial branches (brachiocephalic artery or BA, LCCA or left common carotid artery, and LSA of left subclavian artery), PA, MPA, and DAO were obtained (Tables 1, 2 and 3), including the PI, RI, VTI, PSV, S/D, diameter, isthmus displacement, Z-score, flow velocity, flow volume, LCO, CCO, and ratios between different parameters.

Most of the ultrasound parameters were significantly (P<0.05) correlated with the gestational age (Figs. 2, 3 and 4 and supplemental Figs. 1–8). The ratios of the MCA data to those of the UA both inside and outside the fetal abdomen, of the right to the left atrium or ventricle, and of the isthmus diameter and flow volume to those of the

DA, aorta, AAO, DAO, and arch branches remained relatively stable (Figs. 1, 2 and 3). A significant (P<0.05) negative correlation with the gestational age was detected in the intra-abdominal and free UA parameters (S/D, PI and RI) (Supplemental Fig. 1). Although significant (P<0.05), a relatively stable correlation with the gestational age was detected in the parameters of fetal weight%, MCA S/D, PI and RI (Supplemental Fig. 1), intra-abdominal UA PSV and VTI, fetal cardio-thoracic ratio (Supplemental Fig. 2), MV- and TV-E/A (Supplemental Fig. 3), isthmus Z-score and displacement (Supplemental Fig. 4), BA-LCCA and LCCA-LSA distance, Z-score of aorta, AAO, PA, MPA, and DAO (Supplemental Fig. 5).

A significant (P<0.05) positive correlation with the gestational age was detected in the fetal biological data (Supplemental Fig. 1), MCA PSV and VTI (Supplemental Fig. 1), free-UA PSV, VTI and perimeter ratio (Supplemental Fig. 2), left and right atrium and ventricle, MV- and TV-E, TV-A, DA and isthmus diameter (Supplemental Figs. 3 and 4), aortic arch and arch branch diameter (Supplemental Fig. 4), aortic diameter and flow volume and velocity, AAO diameter and VTI, PA and MPA diameter (Supplemental Fig. 5), MPA PSV and VTI, DAO parameters (diameter, flow velocity and volume, VTI, and PSV) (Supplemental Fig. 6), isthmus flow volume and velocity, PA flow volume, DA and BA parameters (flow volume, PSV and VTI) (Supplemental Figs. 7 and 8), LCCA and LSA parameters (flow volume, PSV, and VTI) (Supplemental Fig. 8).

The right atrium and ventricle were significantly (P<0.05) greater than the left atrium (1.27±0.35 vs. 1.17±0.29 cm, P<0.001) and ventricle (1.18±0.34 vs. 1.17±0.31 cm, P=0.001), respectively (Table 1). The PA/AAO diameter ratio was 0.91–1.45(1.15±0.09). The LCO (AO flow volume) was significantly smaller than the RCO (PA flow volume) (329.37±193.87 ml vs. 430.46±275.39 ml, P<0.001). The LCO was in a significant (P<0.05) positive correlation with RCO, CCO, and the flow volume of BA, LCCA, LSA, isthmus, and DAO, whereas the RCO was significantly positively correlated with the CCO and the flow volume of DA and DAO (Fig. 5). In normal condition, the RCO contributed more to the CCO and DAO flow volume, whereas the LCO contributed more to the isthmus flow volume.

Discussion

In this study exploring the normal range and distribution trend of ultrasound parameters with the gestational age in normal fetuses, a certain correlation was found in the ultrasound parameters of normal fetuses with the gestational age, and the ratios among different parameters remained relative stable. These findings could be used for determination of abnormal growth of the fetuses in prenatal ultrasound scan.

Table 1 Biological, MCA, UA, and cardiac data

Variables	Data	Variables	Data
Pregnant women no.	417	MCA/intra-UA PSV	0.26–1.93(0.70±0.28)
Pregnant women age (y)	19–42 (30.2±3.9)	MCA/intra-UA S/D	0.29–4.39(1.50±0.54)
GA (w)	20–40 (29.76±5.71)	MCA/intra-UA PI	0.61–3.75(1.56±0.44)
BPD (cm)	0.84–10.2 (7.47±1.52)	MCA/intra-UA RI	0.73–1.88(1.17±0.19)
HC (cm)	17.03–36.01 (27.02±5.1)	MCA /intra-UA VTI	0.09–1.56(0.53±0.22)
AC(cm)	14.58–39.16 (25.51±6.31)	MCA /free-UA PSV	0-2.24(0.96±0.28)
FL (cm)	3.15–7.83 (5.58±1.28)	MCA/ free-UA S/D	0.69–5.63(1.77±0.54)
HL (cm)	2.95–6.89 (4.98±1.02)	MCA /free-UA PI	0.65–3.25(1.74±0.44)
Estimated weight (g)	49.8–4553(1687.32±1087.49)	MCA/free-UA RI	0.87–2.11(1.27±0.19)
Weight%	9.4–99(47.32±20.78)	MCA/free-UA VTI	0.48–3.62(1.43±0.43)
MCA PSV(cm/s)	17.97–94.06(43.44±14.71)	cardiac axis(°)	22.75–57.84(34.83±6.48)
MCA S/D	2.23–10.03(4.62±1.16)	HCR	0.19–0.42(0.28±0.03)
MCA PI	0.74–2.59(1.60±0.30)	HC Perimeter ratio	0.45–0.59(0.53±0.03)
MCA RI	0.55–1.37(0.77±0.07)	Left atrium(cm)	0.59–2.01(1.17±0.29)
MCA VTI(cm)	3.59–21.19(8.87±3.59)	Right atrium(cm)	0.58–2.32(1.27±0.35)
Intra-UA PSV(cm/s)	24.73–114.97(64.77±13.45)	Right atrium/left atrium	0.80–1.47(1.09±0.09)
Intra-UA S/D	1.76–10.18(3.40±1.19)	LV(cm)	0.55–2.08(1.17±0.31)
Intra-UA PI	0.56–1.91(1.08±0.26)	RV(cm	0.57–2.23(1.18±0.34)
Intra-UA RI	0.43–0.94(0.67±0.10)	RV/LV	0.81–1.37(1.01±0.08)
Intra-UA VTI(cm)	5.6-38.21(17.12±4.24)	MV-E(cm/s)	19.37–60.08(36.77±7.03)
Free-UA PSV(cm/s)	21.13–87.42(45.59±9.97)	MV-A(cm/s)	31.8-84.48(53.62±8.33)
Free-UA S/D	1.54–4.47(2.72±0.56)	MV-E/A	0.46–1.16(0.69±0.10)
Free-UA PI	0.44–1.5(0.95±0.19)	TV-E(cm/s)	17.95–74.76(43.86±8.76)
Free-UA RI	0.35–0.78(0.62±0.08)	TV-A(cm/s)	16.42–89.18(60.50±9.25)
Free-UA VTI(cm)	5.21–24.34(12.52±3.45)	TV-E/A	0.50–0.93(0.72±0.08)

Note GA, gestational age; BPD, biparietal diameter; HC, head circumference; AC, abdomen circumference; FL, femur length; HL, humerus length; MCA, middle cerebral artery; PSV, peak systolic velocity; S/D, PSV/EDV (end diastolic velocity); PI, pulsatility index; RI, resistance index; VTI, velocity time integral; UA, umbilical artery; Intra- UA, the UA segment inside the fetal abdomen; free-UA, the UA segment outside the fetus before the UA placental insertion; HCR, Heart to chest area ratio; HC, Heart to chest; RV, Right ventricle; LV, left ventricle; MV-E, Mitral valve E-peak flow velocity; MV-A, mitral valve A-peak flow velocity; TV-E, tricuspid valve E peak; TV-A, tricuspid valve A peak. Data were presented as mean and standard deviation if in the normal distribution. Data were presented as mean±standard deviation if meeting the normal distribution or as median and interquartile range if not in the normal distribution

In fetuses with prenatal restricted growth, blood flow is redistributed from the peripheral tissues and organs to the brain, and Doppler ultrasound examination of the UA and fetal cerebral arteries (MCA in particular) can be applied to evaluate the relevant changes [16]. In these fetuses, the UA PI is increased while the MCA PI is decreased. The nomograms of the MCA PI and PSV with advanced gestational age have been reported, and decreased MCA PI has been reported in fetuses with congenital heart disease or at risk of perinatal mortality and morbidity [16–19]. Lower MCA PI and cerebral placental ratio (MCA PI/UA PI) and increased UA PI were reported in fetal hypoplastic left heart syndrome and isolated coarctation of the aorta (CoA), and the MCA PI is associated with changed fetal cerebral blood flow and positively correlates with head development [20]. The MCA PSV has been found to increase as a good indicator for perinatal mortality in a group of fetuses with restricted growth [16, 21]. Our study provided the ultrasound parameters of fetal biology, MCA and UA both inside and outside the fetal abdomen of normal fetuses as references to diagnose potential abnormalities of fetal growth. The fetal biparietal diameter, head circumference, abdomenal circumference, femur length, humerus length, estimated body weight positively correlated with the gestational age, and the ratios of the MCA data to those of the UA both inside and outside the fetal abdomen remained relatively stable during the 20–40 week gestaion investigated in our study.

The Prenatal Growth Assessment Score (PGAS) has been developed to detect different kinds of fetal growth issues except those of tissue abnormalities [22], and the PGAS was based on the head circumference, abdominal circumference, femur diaphysis length, mid-thigh circumference, and estimated weight. Nonetheless, this score is limited by reference ranges determined from all the 20–40 week gestation data without considering age-specific differences and was initially proposed for only one combination of anatomical parameters [22–24]. Our study provided the reference ranges of the fetuses during the 20–40 weeks and could be used as references for normal growth.

In fetuses suspected of CoA, the right heart structures (atrium and ventricle) are larger than the left

Table 2 Data of DA, isthmus, aorta, aortic arch, arch arteries, and pulmonary artery

Variables	Data	Variables	Data
DA diameter (cm)	0.16–0.76(0.37 ± 0.14)	LCCA-LSA/arch 3 diameter	0.09–1.64(0.55 ± 0.26)
3VTV Isthmus diameter(cm)	0.18–0.59(0.35 ± 0.09)	LCCA-LSA/BA-LCCA	0.36–7.6(1.71 ± 0.81)
SV Isthmus diameter(cm)	0.15–0.55(0.32 ± 0.08)	AO diameter(cm)	0.21–0.79(0.44 ± 0.12)
SV Isthmus ZS	-6.03- 2.65(-1.21, 0.49)	AO-ZS	-2.81-1.25(-0.76,0.83)
3VTV Isthmus/DA	0.52–1.52(0.99 ± 0.16)	AAO(cm)	0.22–0.8(0.47 ± 0.13)
SV Isthmus/DA	0.42–1.52(0.91 ± 0.17)	AAO-ZS	-3.44-0.68(-1.26 ± 0.62)
3VTV Transverse arch diameter(cm)	0.19–0.73(0.42 ± 0.12)	AO flow velocity(cm/s)	56.31-136.78(91.86 ± 13.58)
Arch diameter 1(cm)	0.12–0.82(0.47 ± 0.12)	AO VTI(cm)	8.03–19.52(13.29 ± 1.95)
Arch diameter 2(cm)	0.09–0.68(0.36 ± 0.10)	AO flow volume (ml/min)	49.63-1170.47(306.86, 288.5)
Arch diameter 3(cm)	0.09–0.67(0.35 ± 0.09)	AO flow/weight(ml/ min/g)	0.11–9.79(0.21,0.06)
Arch diameter 3/2	0.68–1.5(0.96 ± 0.08)	PA (cm)	0.28–0.99(0.54 ± 0.15)
SV Isthmus /arch 1 diameter	0.48–1.67(0.69 ± 0.10)	PA-ZS	-3.23-0.97(-0.92,0.87)
SV isthmus /arch 2 diameter	0.63–2.22(0.90 ± 0.14)	MPA(cm)	0.33–1.32(0.73 ± 0.22)
SV Isthmus /arch diameter 3	0.65–2.22(0.93 ± 0.13)	MPA-ZS	-1.92-2.37(0.74, 0.91)
SV isthmus diameter/AAD	0.47–0.92(0.69 ± 0.07)	MPA PSV(cm/s)	42.38–99.79(68.60 ± 10.84)
SV isthmus diameter/AD	0.47-1(0.73 ± 0.08)	PA VTI(cm)	6.72–17.33(11.47 ± 2.02)
3D LSA-DAO displacement (cm)	0.09–34.5(0.39 ± 1.68)	PA flow volume(ml/min)	65.57-1344.22(377.52,430)
3D STIC Isthmus/DA angle (°)	0.33–68.32(24.44 ± 9.96)	PA flow volume/ weight (ml/min /g)	0.13–14.51(0.30 ± 0.71)
3D HD live flow DA-Isthmus angle (above view) (°)	8.45–79.86(27.82 ± 8.36)	AO flow /PA flow	0.01–1.34(0.81 ± 0.16)
3D HD live flow DA- Isthmus (SV)(°)	6.65–68.63(24.52 ± 10.02)	CCO(ml/min)	115.77-2514.69(674.72, 702)
BA(cm)	0.09–0.49(0.24 ± 0.08)	CCO/weight(ml/min/g)	0.25–24.32(0.47,0.11)
LCCA(cm)	0.09–0.46(0.19 ± 0.07)	PA/AAO	0.91–1.45(1.15 ± 0.09)
LSA(cm)	0.06–0.37(0.19 ± 0.06)	PA/AO	1-13.42(1.24 ± 0.60)
BA-LCCA distance(cm)	0.04–0.34(0.12 ± 0.05)	MPA/AAO	0.95–2.06(1.55 ± 0.18)
LCCA-LSA distance(cm)	0.04–0.52(0.18 ± 0.09)		

Note DA, ductus arteriosus; 3VTV, 3 vessel trachea view; SV, sagittal view; ZS, Z-score; isthmus, aortic isthmus; AAD, ascending aortic inner diameter; AD, aortic inner diameter; 3D, HD live flow image; DAO, descending aorta; LSA-DAO, left subclavian artery-descending aorta; BA, brachiocephalic artery trunk; LCCA, left common carotid artery; AO, aorta; AAO, ascending aorta; VTI, velocity time integral; PA, pulmonary artery; MPA, main pulmonary artery; PSV, peak systolic velocity; CCO, combined cardiac output; AO flow volume indicates the left cardiac output; PA flow volume indicates the right cardiac output. Data were presented as mean ± standard deviation if meeting the normal distribution or as median and interquartile range if not in the normal distribution

ones, the TV is larger than the MV, and the PA/AAO diameter ratio is greater than 1.60 at the 3VTV view, with the presence of a narrowed aortic isthmus, hypoplastic transverse aortic arch, and CoA shelf [25–27]. Transverse aortic arch hypoplasia and elevated PA valve and PA diameters have also been reported in neonates with CoA, which may suggest reduced aortic arch flow and raised PA and DA flow in fetuses [28]. In our study, normal fetuses showed greater right heart structures than the left ones, but a smaller ratio of the PA/AAO diameter (range 0.91–1.45 and mean 1.15 ± 0.09), with no presence of CoA shelf, hypoplastic transverse aortic arch, or a narrowed isthmus. The right heart structures are larger than the left ones because the major blood flow of the fetus comes from the right heart. A prenatal definitive diagnosis of congenital fetal diseases like CoA can influence and decrease the mortality rate [26, 29]. Definition of the normal ultrasound parameters is helpful for detection of possible congenital fetal diseases. Antenatal ultrasound parameters have been applied for the diagnosis of CoA [30–35],

including diameter of the PA or the aorta at the aortic valve, aortic isthmus, and AAO, and a ratio between the DA and aortic isthmus. The Z-scores of the aortic isthmus and AAO had been reported to be significantly lower in neonates with CoA [36, 37]. The MPA and TV Z-scores significantly rose while the mean Z-scores of the MV and the aortic isthmus significantly dropped in CoA fetuses [30]. A significant increase in the LCCA-LSA distance and aortic arch-DAO angle was also reported in CoA positive fetuses [38]. In our study, these ultrasound parameters were investigated in normal fetuses and can be used as references for detection of potential diseases.

Cardiac remodeling manifests as alterations in mass, size, geometry, and function of the heart in response to injury or load [9, 39]. This process can cause impairment in the cardiac ejection and/or relaxation ability as clinical or subclinical cardiac dysfunction. Cardiac structure dysfunction and remodeling have been described in some antenatal conditions but are scarcely described in fetuses with congenital heart diseases [9,

Table 3 Data of cardiac output, PA, aorta, isthmus, and DA

Variables	Data	Variables	Data
3VTV Isthmus/ DAO	0.53–0.96(0.76 ± 0.08)	Isthmus diastolic velocity(cm/s)	7.22–66.82(23.47 ± 8.05)
SV Isthmus/ DAO	0.44–0.96(0.70 ± 0.08)	Isthmus diastolic VTI(cm)	0.77–7.2(3.39 ± 0.89)
SV Isthmus /DA	0.42–1.52(0.91 ± 0.17)	Isthmus Diastolic flow volume(ml/min)	3.21-206.45(43.76 ± 27.17)
3VTV Isthmus/ DA	0.52–1.52(0.99 ± 0.16)	Isthmus Diastolic flow/weight(ml/min/g)	0.003-1.60(0.03, 0.13)
DAO-ZS	-2.32-2.75(-0.25, 0.88)	Isthmus diastolic /systolic VTI	0.14–1.26(0.37 ± 0.09)
DAO diameter(cm)	0.23–0.84(0.47 ± 0.13)	Isthmus diastolic /isthmus total VTI	0.12–0.53(0.27 ± 0.04)
DAO velocity(cm/s)	41.8-180.11(99.88 ± 25.42)	Isthmus/AO flow	0.15–1.12(0.51 ± 0.13)
DAO VTI(cm)	6.29–29.69(16.43 ± 4.10)	Isthmus flow/CCO	0.003–0.43(0.23 ± 0.06)
DAO flow volume(ml/min)	46.68-1826.69(397.14, 483.31)	DA PSV(cm/s)	40.92-163.11(99.73 ± 22.11)
DAO flow /weight(ml/min/g)	0.12–25.40(0.27, 0.07)	DA VTI(cm)	6.46–33.14(15.04 ± 3.57)
Isthmus PSV (Total)(cm/s)	32.32-139.71(87.22 ± 16.49)	DA flow(ml/min)	30.22-1268.88(199.17,330.12)
Isthmus VTI(cm)	5.58–20.03(12.63 ± 2.46)	DA flow/weight(ml/min/g)	0.05–7.81(0.15, 0.07)
Isthmus flow volume(ml/min)	15.70-524.94(141.47, 145.15)	BA-PSV(cm/s)	42.72-296.51(102.46 ± 31.33)
Isthmus flow volume/weight(ml/min/g)	0.02–6.41(0.11, 0.04)	BA VTI(cm)	1.73–41.98(11.85 ± 4.68)
Isthmus flow /LCO	0.15–1.12(0.51 ± 0.13)	BA flow(ml/min)	0-501.93(69.63, 104.22)
Isthmus flow volume/CCO	0.003–0.43(0.23 ± 0.06)	BA flow/weight(ml/min/g)	0-3.83(0.05, 0.03)
Isthmus/DA flow volume	0.08–2.06(0.75 ± 0.34)	LCCA PSV(cm/s)	28.95–333.5(98.83 ± 33.47)
Isthmus/DAO flow volume	0.07–0.89(0.39 ± 0.13)	LCCA VTI(cm)	3.05–47.19(11.85 ± 4.85)
Isthmus/BA flow volume	0.33–8.07(2.34 ± 1.21)	LCCA flow(ml/min)	0-292.08(45.67,78.42)
Isthmus/LCCA flow volume	0.48–14.14(3.22, 2.30)	LCCA flow/weight(ml/min/g)	0-2.85(0.03, 0.02)
Isthmus/LSA flow volume	0.66–14.27(3.89 ± 2.12)	LSA PSV(cm/s)	26.38-228.48(98.20 ± 28.78)
Isthmus systolic velocity(cm/s)	32.32-141.49(89.70 ± 16.59)	LSA VTI(cm)	3.74–26.26(11.27 ± 3.52)
Isthmus systolic VTI(cm)	4.84–15.08(9.40 ± 1.95)	LSA flow(ml/min)	0-243.34(43.89, 61.62)
Isthmus Systolic flow volume(ml/min)	13.62-338.66(120.48 ± 69.37)	LSA flow/weight(ml/min/g)	0-2.04(0.03, 0.01)
Isthmus systolic flow volume/weight(ml/min/g)	0.01–5.58(0.08, 0.03)	LSA/isthmus flow	0-1.52(0.33 ± 0.16)

Note PA, pulmonary artery; DA, ductus arteriosus; 3VTV, 3 vessel trachea view; DAO, descending aorta; SV, sagittal view; ZS, Z score; VTI, velocity time integral; PSV, peak systolic velocity; LCO, left cardiac output; CCO, combined cardiac output; BA, brachiocephalic artery trunk; LCCA, left common carotid artery; LSA, left subclavian artery; AO, aorta; MPA, main pulmonary artery; AAO, ascending aorta; DAO, descending aorta; LSA, left subclavian artery; VTI, velocity time integral; PSV, peak systolic velocity. Data were presented as mean±standard deviation if meeting the normal distribution or as median and interquartile range if not in the normal distribution

40]. With the cardiac ultrasound parameters obtained in normal fetuses, correct prenatal diagnosis of some congenital heart diseases can be reached earlier. In normal fetuses, the left ventricle develops under a low volume load and normal pressure condition, and after birth, the left ventricle changes to a globular shape and the filling velocities are increased because of elevated pulmonary venous return and closed foramen ovale to support the system flow. This is why the left cardiac structures, including the atrium and ventricle, were significantly smaller than the right ones in the normal fetuses as revealed by our study. This significant difference between the right and left cardiac structures may require to reach a certain degree for the diagnosis of a diseased status. Our study also found that the LCO was significantly smaller than the RCO (329.37 ± 193.87 ml vs. 430.46 ± 275.39 ml, *P* < 0.001), with the RCO contributing more to the CCO and DAO flow volume while the LCO contributing more to the isthmus flow volume.

This study had some limitations such as a relatively small cohort of fetuses, Chinese subjects enrolled only, one-center study design, and no control, which may all result in publication bias and affect the generalization of the outcome. Future prospective, multi-center studies with a lot of fetuses enrolled and multiple races and ethnicities involved will have to be conducted for better outcomes.
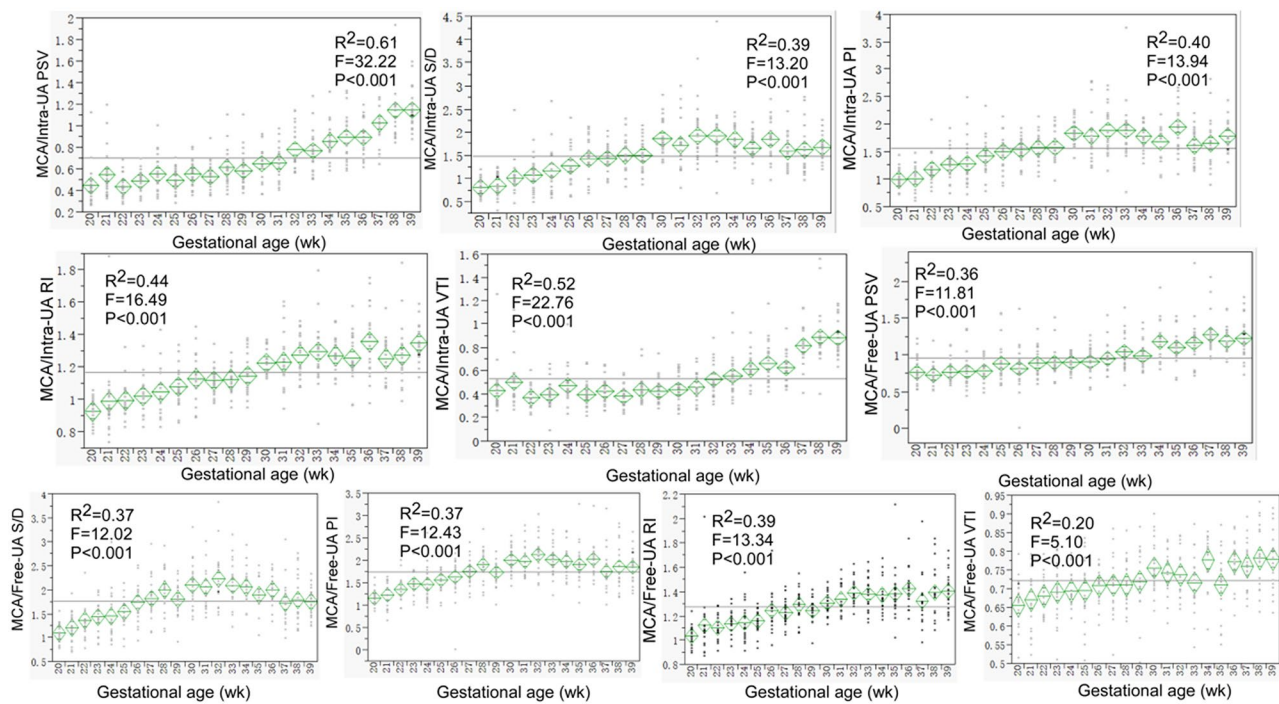
Fig. 2 Trends of the ratios of the fetal MCA (middle cerebral artery) parameters to those of the intra-abdominal and free UA (umbilical artery) were shown with the gestational age. These ratios were in a narrow relatively-stable range
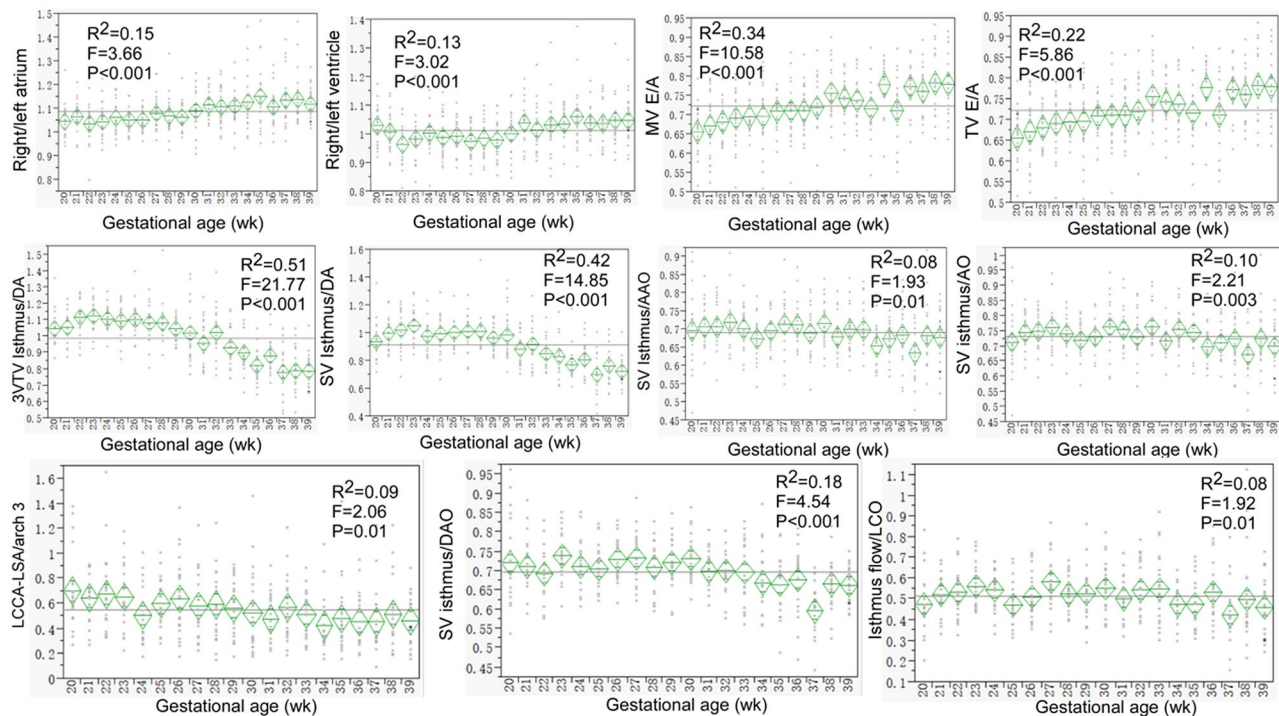

Fig. 3 The trends with the gestational age were demonstrated in the ratios of between the right and left atrium and ventricle, MV (mitral valve)- and TV (tricuspid valve)-E/A peak flow velocity, ratio of isthmus to ductus arteriosus (DA), aorta, AAO and DAO diameter, ratio of LCCA-LSA distance to arch 3 diameter, and isthmus flow volume to the left cardiac output (LCO). These ratios were relatively stable
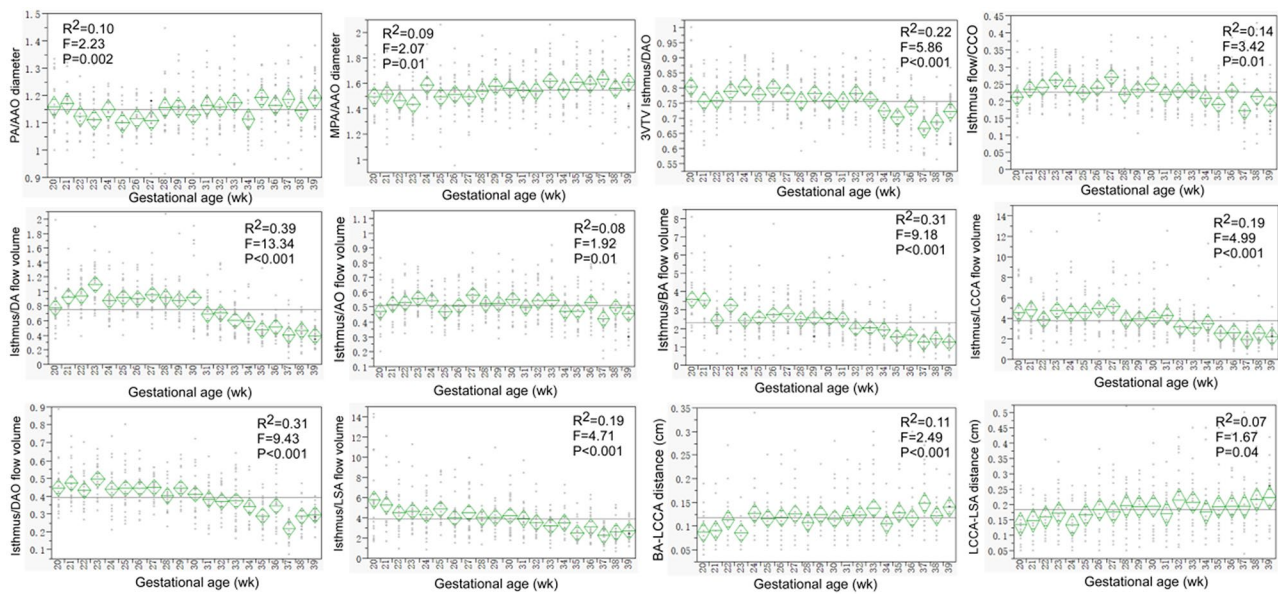
Fig. 4 Relative stable trends with the gestational age were demonstrated in the ratios of the pulmonary artery (PA) and main pulmonary artery (MPA) to the ascending aorta (AAO) and descending aorta (DAO) diameter, of the isthmus flow volume to that of left cardiac output (LCO), combined cardiac output (CCO), ductus arteriosus (DA), aorta (AO), brachiocephalic artery (BA), left common carotid artery (LCCA), DAO, and left subclavian artery (LSA), and the BA-LCCA or LCCA-LSA distance
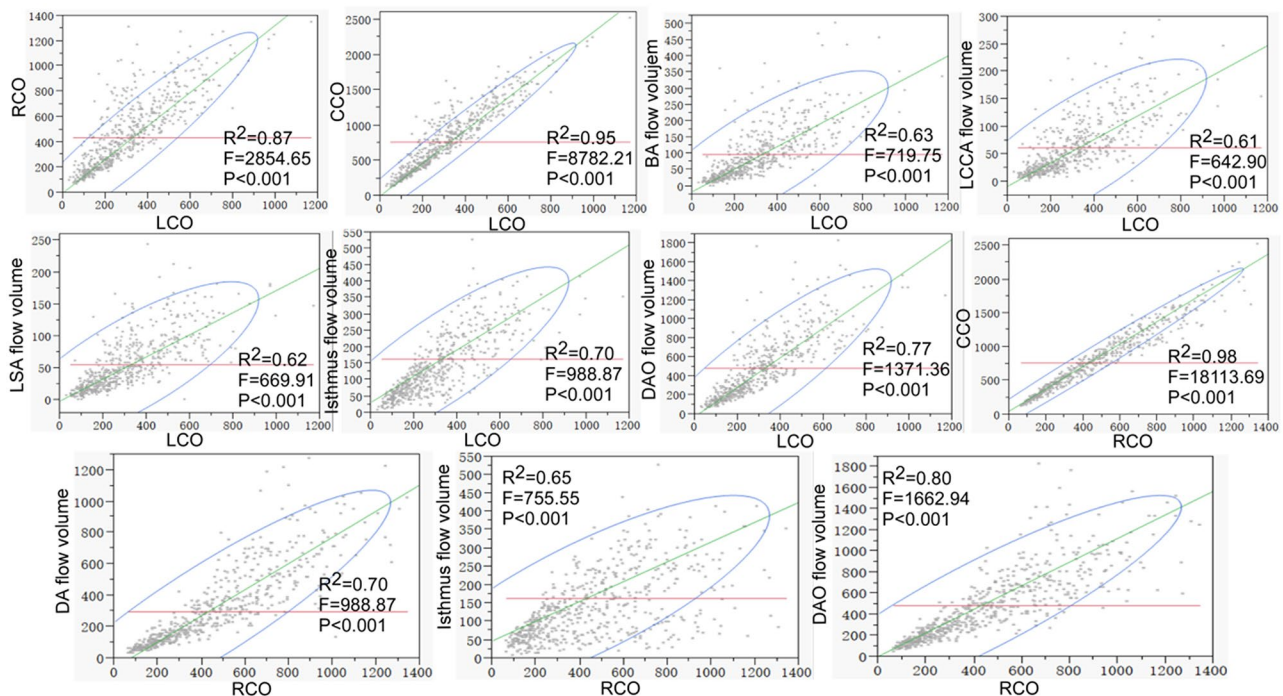

Fig. 5 The left cardiac output (LCO) was in a significant ($P < 0.05$) positive correlation with right cardiac output (RCO), combined cardiac output (CCO), and the flow volume of brachiocephalic artery (BA), left common carotid artery (LCCA), left subclavian artery (LSA), isthmus, and descending aorta (DAO), and the RCO was significantly positively correlated with the CCO and the flow volume of ductus arteriosus (DA) and DAO. In normal condition, the RCO contributed more to the CCO and DAO flow volume, whereas the LCO contributed more to the isthmus flow volume

Conclusion

In summary, a certain correlation exists in the ultrasound parameters of normal fetuses with the gestational age, and the ratios among different parameters remain relative stable. The right heart structures are significantly larger than the left ones in normal fetuses, with the right cardiac output contributing more to the CCO and DAO flow volume while the left cardiac output contributing more to the isthmus flow volume. These findings can be used for determination of abnormal growth of the fetuses in prenatal ultrasound scan.

Abbreviations

2D	Two dimension
3D	Three dimension
PSV	Peak systolic velocity
PI	Pulsatility index
RI	Resistance index
S/D	Peak systolic velocity/peak diastolic velocity
VTI	Velocity time integral
MCA	Middle cerebral artery
UA	Umbilical artery
MV-A	Mitral valve A peak flow velocity
TV-E	Tricuspid valve E peak flow velocity
AO	Aorta
AAO	Ascending aorta
MPA	Main pulmonary artery
PA	Pulmonary artery
LCO	Left cardiac output
RCO	Right cardiac output
CCO	Combined cardiac output
DA	Ductus arteriosus
3VTV	3 vessel tracheal view
DAO	Descending aorta
LCCA	Left common carotid artery
BA	Brachiocephalic artery
LSA	Left subclavian artery
CoA	Coarctation of the aorta
PGAS	Prenatal growth assessment score
GA	Gestational age
BPD	Biparietal diameter
HC	Head circumference
AC	Abdomen circumference
FL	Femur length
HL	Humerus length
SV	Sagittal view
ZS	Z-score
AAD	Ascending aortic inner diameter
AD	Aortic inner diameter
SVC	Superior vena cava
ISTH	Aortic isthmus

Supplementary Information

The online version contains supplementary material available at https://doi.org/10.1186/s12947-024-00328-w.

> Supplementary Material 1

Author contributions

Study design: Guihong Chen, Jie Mi; Data collection: Guihong Chen, Pin Wang, Yanhong Zhang, Na Li, Liman Fu, Yu Chen1, Xuna Geng, Yongfeng Han, Lu Qin; Data analysis: Guihong Chen, Bulang Gao; Supervision: Guihong Chen, Tianxiao Yu; Approval: All authors.

Declarations

Competing interests

The authors declare no competing interests.

Author details

¹Department of Medical Ultrasound, Research Center for Clinical Medicine Sciences, The Fourth Hospital of Shijiazhuang, No.16 Tangu North Street, Shijiazhuang 050000, Hebei Province, China
²Cardiology Department, Shijiazhuang People's Hospital, No. 365, Jianhua South Street, Shijiazhuang 050000, Hebei Province, China

References

1. Deter RL, Dicker P, Lee W, Tully EC, Cody F, Malone FD, Flood KM. Growth patterns and cardiovascular abnormalities in SGA fetuses: 2. Normal growth and progressive growth restriction. J Matern Fetal Neonatal Med. 2022;35(14):2818–27.
2. Deter RL, Lee W, Dicker P, Tully EC, Cody F, Malone FD, Flood KM. Third-trimester growth diversity in small fetuses classified as appropriate-for-gestational age or small-for-gestational age at birth. Ultrasound Obstet Gynecol. 2021;58(6):882–91.
3. Deter RL, Lee W, Kingdom JCP, Romero R. Fetal growth pathology score: a novel ultrasound parameter for individualized assessment of third trimester growth abnormalities. J Matern Fetal Neonatal Med. 2018;31(7):866–76.
4. Gardosi J. Customized fetal growth standards: rationale and clinical application. Semin Perinatol. 2004;28(1):33–40.
5. Hugh O, Cowan J, Butler E, Gardosi J. Fetal size vs growth: comparative analysis of three models of growth velocity based on third trimester estimated fetal weights for identifying stillbirth risk. Am J Obstet Gynecol 2023.
6. Hugh O, Gardosi J. Fetal weight projection model to define growth velocity and validation against pregnancy outcome in a cohort of serially scanned pregnancies. Ultrasound Obstet Gynecol. 2022;60(1):86–95.
7. Lees CC, Romero R, Stampalija T, Dall'Asta A, DeVore GA, Prefumo F, Frusca T, Visser GHA, Hobbins JC, Baschat AA, et al. Clinical opinion: the diagnosis and management of suspected fetal growth restriction: an evidence-based approach. Am J Obstet Gynecol. 2022;226(3):366–78.
8. Mula C, Hidalgo J, Peguero A, Mazarico E, Martinez J, Figueras F, Meler E. Third-trimester uterine artery Doppler for prediction of adverse outcome in late small-and adequate for-gestational-age fetuses. Minerva Obstet Gynecol. 2023;75(5):440–8.
9. Soveral I, Crispi F, Walter C, Guirado L, Garcia-Canadilla P, Cook A, Bonnin A, Dejea H, Rovira-Zurriaga C, Sanchez, de Toledo J et al. Early cardiac remodeling in aortic coarctation: insights from fetal and neonatal functional and structural assessment. Ultrasound Obstet Gynecol. 2020;56(6):837–849.
10. Stampalija T, Wolf H, Mylrea-Foley B, Marlow N, Stephens KJ, Shaw CJ, Lees CC. authors T-FS: Reduced fetal growth velocity and weight loss are associated with adverse perinatal outcome in fetuses at risk of growth restriction. Am J Obstet Gynecol. 2023;228(1):71 e71-71 e10.
11. Deter RL, Lee W, Sangi-Haghpeykar H, Tarca AL, Yeo L, Romero R. Individualized fetal growth assessment: critical evaluation of key concepts in the specification of third trimester size trajectories. J Matern Fetal Neonatal Med. 2014;27(6):543–51.
12. Deter RL, Lee W, Yeo L, Erez O, Ramamurthy U, Naik M, Romero R. Individualized growth assessment: conceptual framework and practical implementation for the evaluation of fetal growth and neonatal growth outcome. Am J Obstet Gynecol. 2018;218(2S):S656–78.
13. Sherwin E, Deter R, Joudi N, Trepman P, Lee W, El-Sayed YY, Girsen AI, Datoc I, Hintz SR, Blumenfeld YJ. Individualized growth assessment in pregnancies complicated by fetal gastroschisis. J Matern Fetal Neonatal Med. 2022;35(25):6842–52.

14. Deter RL, Lee W, Kingdom J, Romero R. Second trimester growth velocities: assessment of fetal growth potential in SGA singletons. J Matern Fetal Neonatal Med. 2019;32(6):939–46.

15. Deter RL, Lee W, Sangi-Haghpeykar H, Tarca AL, Yeo L, Romero R. Fetal growth cessation in late pregnancy: its impact on predicted size parameters used to classify small for gestational age neonates. J Matern Fetal Neonatal Med. 2015;28(7):755–65.

16. Mari G, Hanif F, Kruger M, Cosmi E, Santolaya-Forgas J, Treadwell MC. Middle cerebral artery peak systolic velocity: a new Doppler parameter in the assessment of growth-restricted fetuses. Ultrasound Obstet Gynecol. 2007;29(3):310–6.

17. Mari G, Deter RL. Middle cerebral artery flow velocity waveforms in normal and small-for-gestational-age fetuses. Am J Obstet Gynecol. 1992;166(4):1262–70.

18. Mari G, Adrignolo A, Abuhamad AZ, Pirhonen J, Jones DC, Ludomirsky A, Copel JA. Diagnosis of fetal anemia with doppler ultrasound in the pregnancy complicated by maternal blood group immunization. Ultrasound Obstet Gynecol. 1995;5(6):400–5.

19. Man T, He Y, Zhao Y, Sun L, Liu X, Ge S. Cerebrovascular hemodynamics in fetuses with congenital heart disease. Echocardiography. 2017;34(12):1867–71.

20. Yamamoto Y, Khoo NS, Brooks PA, Savard W, Hirose A, Hornberger LK. Severe left heart obstruction with retrograde arch flow influences fetal cerebral and placental blood flow. Ultrasound Obstet Gynecol. 2013;42(3):294–9.

21. Ozcan T, Sbracia M, d'Ancona RL, Copel JA, Mari G. Arterial and venous doppler velocimetry in the severely growth-restricted fetus and associations with adverse perinatal outcome. Ultrasound Obstet Gynecol. 1998;12(1):39–44.

22. Deter RL, Stefos T, Harrist RB, Hill RM. Detection of intrauterine growth retardation in twins using individualized growth assessment: I. evaluation of growth outcome at birth. J Clin Ultrasound. 1992;20(9):573–7.

23. Deter RL, Lee W, Sangi-Haghpeykar H, Tarca AL, Yeo L, Romero R. A modified prenatal growth assessment score for the evaluation of fetal growth in the third trimester using single and composite biometric parameters. J Matern Fetal Neonatal Med. 2015;28(7):745–54.

24. Hata T, Deter RL, Hill RM. Individual growth curve standards in triplets: prediction of third-trimester growth and birth characteristics. Obstet Gynecol. 1991;78(3 Pt 1):379–84.

25. Slodki M, Rychik J, Moszura T, Janiak K, Respondek-Liberska M. Measurement of the great vessels in the mediastinum could help distinguish true from false-positive coarctation of the aorta in the third trimester. J Ultrasound Med. 2009;28(10):1313–7.

26. Slodki M, Rizzo G, Augustyniak A, Seligman NS, Zych-Krekora K, Respondek-Liberska M, International Prenatal Cardiology Collaboration G. Retrospective cohort study of prenatally and postnatally diagnosed coarctation of the aorta (CoA): prenatal diagnosis improve neonatal outcome in severe CoA. J Matern Fetal Neonatal Med. 2020;33(6):947–51.

27. Akalin M, Demirci O, Yucel IK, Erol N. Fetal echocardiographic findings to Predict Early Surgical repair and neonatal outcomes in fetuses with isolated Coarctation of the Aorta. Am J Perinatol 2022.

28. Morrow WR, Huhta JC, Murphy DJ Jr., McNamara DG. Quantitative morphology of the aortic arch in neonatal coarctation. J Am Coll Cardiol. 1986;8(3):616–20.

29. Polyviou S, Charakida M, Miller OI, Rscn TW, Vigneswaran TV, Zidere V, Day TG, Lloyd DFA, Sharland GK, Simpson JM. Outcome and impact of Associated Left-Sided Cardiac lesions in Coarctation of the Aorta diagnosed during fetal life. Am J Cardiol. 2022;166:114–21.

30. Familiari A, Morlando M, Khalil A, Sonesson SE, Scala C, Rizzo G, Del Sordo G, Vassallo C, Elena Flacco M, Manzoli L, et al. Risk factors for Coarctation of the aorta on prenatal Ultrasound: a systematic review and Meta-analysis. Circulation. 2017;135(8):772–85.

31. Lee A, Reddy M, Chai M, Grange Sobe I, Green E, Rolnik DL, Rao SJV, Teoh M. Subjective and objective Sonographic Assessment for the prenatal detection of neonatal coarctation of the Aorta. Fetal Diagn Ther. 2023;50(2):98–105.

32. Matsui H, Mellander M, Roughton M, Jicinska H, Gardiner HM. Morphological and physiological predictors of fetal aortic coarctation. Circulation. 2008;118(18):1793–801.

33. Power A, Nettel-Aguirre A, Fruitman D. Fetal right ventricular prominence: Associated Postnatal Abnormalities and Coarctation Clinical Prediction Tool. Pediatr Cardiol. 2017;38(7):1471–7.

34. Jowett V, Aparicio P, Santhakumaran S, Seale A, Jicinska H, Gardiner HM. Sonographic predictors of surgery in fetal coarctation of the aorta. Ultrasound Obstet Gynecol. 2012;40(1):47–54.

35. Anuwutnavin S, Satou G, Chang RK, DeVore GR, Abuel A, Sklansky M. Prenatal Sonographic predictors of neonatal coarctation of the Aorta. J Ultrasound Med. 2016;35(11):2353–64.

36. Contro E, Cattani L, Balducci A, Prandstraller D, Perolo A, Larcher L, Reggiani MLB, Farina A, Donti A, Gargiulo GD, et al. Prediction of neonatal coarctation of the aorta at fetal echocardiography: a scoring system. J Matern Fetal Neonatal Med. 2022;35(22):4299–305.

37. Wang H, Lei W, Liu J, Yang B, Li H, Huang D. The diastolic and systolic velocity-time integral ratio of the aortic isthmus is a sensitive Indicator of aortic coarctation in fetuses. J Am Soc Echocardiogr. 2019;32(11):1470–6.

38. Arya B, Bhat A, Vernon M, Conwell J, Lewin M. Utility of novel fetal echocardiographic morphometric measures of the aortic arch in the diagnosis of neonatal coarctation of the aorta. Prenat Diagn. 2016;36(2):127–34.

39. Cohn JN, Ferrari R, Sharpe N. Cardiac remodeling–concepts and clinical implications: a consensus paper from an international forum on cardiac remodeling. Behalf of an International Forum on Cardiac Remodeling. J Am Coll Cardiol. 2000;35(3):569–82.

40. Crispi F, Bijnens B, Figueras F, Bartrons J, Eixarch E, Le Noble F, Ahmed A, Gratacos E. Fetal growth restriction results in remodeled and less efficient hearts in children. Circulation. 2010;121(22):2427–36.

Publisher's Note

Terms and Conditions

Springer Nature journal content, brought to you courtesy of Springer Nature Customer Service Center GmbH ("Springer Nature").

Springer Nature supports a reasonable amount of sharing of research papers by authors, subscribers and authorised users ("Users"), for small-scale personal, non-commercial use provided that all copyright, trade and service marks and other proprietary notices are maintained. By accessing, sharing, receiving or otherwise using the Springer Nature journal content you agree to these terms of use ("Terms"). For these purposes, Springer Nature considers academic use (by researchers and students) to be non-commercial.

These Terms are supplementary and will apply in addition to any applicable website terms and conditions, a relevant site licence or a personal subscription. These Terms will prevail over any conflict or ambiguity with regards to the relevant terms, a site licence or a personal subscription (to the extent of the conflict or ambiguity only). For Creative Commons-licensed articles, the terms of the Creative Commons license used will apply.

We collect and use personal data to provide access to the Springer Nature journal content. We may also use these personal data internally within ResearchGate and Springer Nature and as agreed share it, in an anonymised way, for purposes of tracking, analysis and reporting. We will not otherwise disclose your personal data outside the ResearchGate or the Springer Nature group of companies unless we have your permission as detailed in the Privacy Policy.

While Users may use the Springer Nature journal content for small scale, personal non-commercial use, it is important to note that Users may not:

1. use such content for the purpose of providing other users with access on a regular or large scale basis or as a means to circumvent access control;

2. use such content where to do so would be considered a criminal or statutory offence in any jurisdiction, or gives rise to civil liability, or is otherwise unlawful;

3. falsely or misleadingly imply or suggest endorsement, approval , sponsorship, or association unless explicitly agreed to by Springer Nature in writing;

4. use bots or other automated methods to access the content or redirect messages

5. override any security feature or exclusionary protocol; or

6. share the content in order to create substitute for Springer Nature products or services or a systematic database of Springer Nature journal content.

In line with the restriction against commercial use, Springer Nature does not permit the creation of a product or service that creates revenue, royalties, rent or income from our content or its inclusion as part of a paid for service or for other commercial gain. Springer Nature journal content cannot be used for inter-library loans and librarians may not upload Springer Nature journal content on a large scale into their, or any other, institutional repository.

These terms of use are reviewed regularly and may be amended at any time. Springer Nature is not obligated to publish any information or content on this website and may remove it or features or functionality at our sole discretion, at any time with or without notice. Springer Nature may revoke this licence to you at any time and remove access to any copies of the Springer Nature journal content which have been saved.

To the fullest extent permitted by law, Springer Nature makes no warranties, representations or guarantees to Users, either express or implied with respect to the Springer nature journal content and all parties disclaim and waive any implied warranties or warranties imposed by law, including merchantability or fitness for any particular purpose.

Please note that these rights do not automatically extend to content, data or other material published by Springer Nature that may be licensed from third parties.

If you would like to use or distribute our Springer Nature journal content to a wider audience or on a regular basis or in any other manner not expressly permitted by these Terms, please contact Springer Nature at

onlineservice@springernature.com